Three-Phase Relative Permeability of Water-Wet, Oil-Wet, and Mixed-Wet Sandpacks

D.A. DiCarlo, SPE, **Akshay Sahni,** SPE,* and **M.J. Blunt,**** SPE, Stanford U.

Summary

We study three-phase flow in water-wet, oil-wet, mixed-wet, and fractionally wet sandpacks. We make the mixed-wet pack by invading a water-filled water-wet pack with crude oil and aging it for a week. This process mimics wettability changes in reservoir settings, leading to a realistic arrangement of wettability at the pore scale. We characterize the wettability of each sand pack by measuring the capillary pressure curves. We obtain the oil and water relative permeabilites during three-phase gravity drainage, by measuring the saturation in situ using computerized tomography scanning. In an analog experiment, we measure pressure gradients in the gas phase to obtain the gas relative permeability. Thus we determine all three relative permeabilities as a function of saturation for each wettability. We find that under uniform wetting, the relative permeabilities of the most-wetting phase (water in a water-wet pack, oil in an oil-wet pack) are similar. However, the relative permeabilities of the intermediate-wet phase (oil in a water-wet pack, water in a oil-wet pack) are very different at low saturations, with spreading oils showing a characteristic layer drainage regime. The mixed-wet pack also shows the layer drainage regime. We also find that the gas relative permeability is smaller in an oil-wet medium than in a water-wet medium. We explain the observations in terms of wetting, spreading, and the pore scale configurations of fluid.

Introduction

A knowledge of three-phase (water, oil, and gas) flow in porous media is essential for predicting enhanced oil recovery and the migration of nonaqueous phase pollutants. In oil reservoirs, three-phase flow will occur during gas injection, gas cap expansion, and thermal flooding among other processes.

In two-phase flow, one phase will wet the porous medium more than the other phase. This wetting phase occupies the smaller pores, crevices, and corners while the nonwetting phase occupies the larger pores with the exact arrangement determined by the capillary pressure. Regardless of which pair of fluids is used (gas/water, oil/water, gas/oil) positioning of the fluids is likely to be similar at the same saturations. In contrast, for three-phase flow there will be an intermediate-wetting phase which will be positioned uniquely in the porous medium, and will affect macroscopic properties such as relative permeability and residual saturation.

We measure three-phase relative permeabilities during the gravity driven displacement of oil and water by gas, which is called gravity drainage. This is an important three-phase process that occurs during gas cap expansion in an oil reservoir and when nonaqueous phase pollutants migrate through an unsaturated soil. Gravity drainage is also relatively easy to study experimentally and its analysis avoids consideration of hysteresis effects, which can be very significant in three-phase flow.[1,2]

Several authors[3-5] have shown that low oil saturations can be reached during three-phase displacements. Most experiments have been performed on uniformly water-wet media (see Ref. 6 for a review). Oak *et al.*[7] studied three-phase relative permeabilities in an intermediate-wet Berea sandstone. Vizika and Lombard[8] studied three-phase drainage for water-wet, oil-wet, and fractionally wet systems. Jerauld[9] developed a model for three-phase relative permeability based on two-phase measurements for Prudhoe Bay, which is a mixed-wet reservoir.

Sahni *et al.*[10] used computerized tomography (CT) scanning to measure oil and water relative permeability in water-wet media and studied the effect of the spreading coefficient. Zhou and Blunt[11] performed three-phase gravity drainage in fractionally wet sandpacks. They measured the saturation distribution at the end of drainage and interpreted the results in terms of the pore scale arrangement of fluid. DiCarlo *et al.*[12] measured three-phase relative permeabilities for oil-wet and fractionally wet packs.

The fractionally wet media studied in the literature were composed of mixtures of oil-wet and water-wet grains. While this is a convenient way of varying the wettability, it does not necessarily represent the real distribution of wettability in a natural setting. An alternative approach is to mimic a physical sequence of wettability changes in the laboratory, which leads to a medium whose pore-scale pattern of wettability represents reservoir rocks. This is achieved by flooding a water-wet water-filled pack with a crude oil and then aging it for several days. This induces a wettability change on the sand surfaces that have come into contact with the oil (see, for example, Ref. 13). Smaller pores that are water filled and the corners of the pore space will remain water-wet. We will call such systems mixed wet.

In this article we extend the work of Sahni *et al.*[10] and of DiCarlo *et al.*[12] to mixed-wet media. The description of the experiments follows that of DiCarlo *et al.*[12] and, for the sake of completeness, we present all our results in water-wet, oil-wet, fractionally wet, and mixed-wet media. We characterize the wettability by measuring two-phase (water/oil) capillary pressure curves. We measure the gas relative permeability using an analog experiment in which we directly measure the gas saturation and pressure gradient. Thus we obtain all three permeabilities for three-phase gravity drainage, in water-wet, oil-wet, mixed-wet, and fractionally wet sandpacks. We explain the results in terms of the pore-scale fluid arrangements.

Materials and Methods

We chose sandpacks as our porous media because they are easy to characterize and they can be easily sectioned for destructive saturation measurements. We used clean industrial sand (No. 60, Corona Industrial Sand Co., Corona, CA) which was initially water-wet. The sand was put through a size 120 sieve to remove any fine particles. We made 15 kg of the sand oil-wet by soaking initially dry sand in a mixture of 20% crude oil (Thums Inc., Long Beach, CA) and 80% iso-octane for 24 hours.[14] This oil-wet sand was then rinsed with iso-octane and air dried. The fractionally wet sand was a 50-50 mixture of the oil and water-wet sands.

Mixed-wet sandpacks were created from water-wet packs, first by saturating the pack with a 0.01 M NaBr brine (pH 4).[14] We then displaced the brine with five pore volumes of the crude/iso-octane mixture, which yielded a pack with a water saturation of $S_w \approx 0.2$. The column was then left to age for a week. After the aging the crude mixture was displaced with iso-octane until the

*Now at Chevron Petroleum Technology Co.
**Now at Imperial College.

This paper (SPE 60767) was revised for publication from paper SPE 49317, prepared for the 1998 SPE Annual Technical Conference and Exihibition in New Orieans, 27–30 September. Original manuscript received for review 19 November 1998. Revised manuscript received 8 October 1999. Manuscript peer approved 8 November 1999.

TABLE 1– FLUID DENSITIES (ρ_w=1069 kg/m^3), VISCOSITIES (μ_w=1.23 cp), AND INTERFACIAL TENSIONS (γ_{gw}=72.0 mN/m)

Oil	ρ_o (kg/m^3)	μ_o (cp)	γ_{ow} (mN/m)	γ_{go} (mN/m)
n-Hexane	659	0.30	50.5	18.0
n-Octane	703	0.51	51.2	21.1
n-Decane	730	0.84	51.4	23.7

effluent ran clear. Finally, the pack was flooded by *n*-octane, replacing the iso-octane, then flooded with the working water phase (either distilled water or 10% NaBr brine, see below) to replace the brine.

For our fluids, we chose *n*-hexane, *n*-octane, or *n*-decane for the oil phase, distilled water or 10% NaBr by weight brine for the water phase, and air for the gas phase. The density of the brine was measured volumetrically, and the density of the oils was taken from the *CRC Handbook*.[15] Viscosities were measured using a viscometer. Interfacial tensions were measured using the pendant drop technique.[16] **Table 1** shows the fluid properties. All experiments were performed at room temperature and pressure.

In all of the experiments, the sandpacks were set to connate water saturation (S_{wc}) or residual oil saturation (S_{or}) by the following procedure. For uniform-wet packs (water-wet and oil-wet), the core was saturated with the most-wetting fluid (water for water-wet, oil for oil-wet) and then displaced with five pore volumes (PV) of the intermediate-wetting fluid (oil or water). This produced an initial condition of S_{wc} for the water-wet pack and S_{or} for the oil-wet pack. The initial conditions of S_{or} for the water-wet pack and S_{wc} for the oil-wet pack were achieved by an additional 5 PV flooding of the most-wetting fluid. For the fractionally wet pack there is no most-wetting fluid, so an initial condition of S_{or} was achieved by flooding a 100% oil-saturated pack with water, and S_{wc} was achieved by flooding a 100% water-saturated pack with oil. For the mixed-wet pack, since its last flood was by the water phase, it is already at S_{or}. An additional flood of oil was used to achieve S_{wc}. For each experiment, a new mixed-wet pack was created from water-wet sand except for the three-phase drainage from S_{wc}. In this case, due to a need to recalibrate the CT scanner, the core that was used for the drainage from S_{or} was dried out completely by flowing dry air through the column for 4 weeks. The column was then filled with oil. This was followed by 2 PV of iso-proponal to miscibly displace the oil, and then 5 PV of brine. Finally, 5 PV of octane was injected to produce the initial condition of S_{wc}. All displacements were performed in a gravitational stable configuration.

Capillary Pressure Curves

To characterize the wettability changes, we measured two-phase water/oil capillary pressure curves using a gravitational equilibrium technique. Distilled water was used for the water phase, and *n*-octane for the oil phase. The desired medium was packed through a continuous pour into a 72 cm column (2.54 cm inner diameter) and sealed at both ends with rubber stoppers. The column consisted of 24 separate 3 cm long polycarbonate sections held together with Teflon shrink tubing, which made it easier for accurate sectioning of the column for saturation measurements. For water injection (which we will call imbibition even for nonwater-wet media), the medium was initially set to S_{wc} (see above). The imbibition began by connecting the bottom of the column to a large tank of water (whose height and thus the water head did not change during the imbibition) and the top to a smaller volumetric tank of oil (whose height changed slightly during the imbibition). Using the calculations described below, the oil and water heads were chosen such that the water would imbibe throughout the porous medium. An identical technique was used for drainage curves (oil invasion), except that the column was initially set to S_{or}, and the heads set for drainage. Thus the curves obtained are for secondary imbibition and secondary drainage.

Once the tanks were attached, the columns were left for roughly 1 week to reach gravitational equilibrium. Then the columns were sectioned, their contents were dropped into a flask containing 25 mL of iso-proponal, and the oil and water saturations were measured using a gas chromatograph (GC). From this we obtained the saturation profile vs. vertical position.

Assuming that we were at capillary equilibrium, the profile can be described in terms of the capillary pressure. We define z positive downward and $z=0$ at the top of the column. Let z_o be the final height of the oil level in the oil tank, and z_w the final height of the water in the water tank. Since we are at equilibrium, the pressure of each phase i as a function of z is given by

$$P_i=\rho_i g(z-z_i), \tag{1}$$

where ρ is the density and g the gravitational constant. Thus the capillary pressure is

$$P_c=P_o-P_w=(\rho_o-\rho_w)gz-(\rho_o gz_o-\rho_w gz_w). \tag{2}$$

The water and oil heads were chosen such that the capillary fringe would be roughly in the center of the column after imbibition. If this did not occur, the experiment was repeated with different heads.

Oil and Water Relative Permeabilities

Before and during gravity drainage, we used a dual energy CT scanner to obtain in-situ measurements of the water and oil saturations.[10] To achieve good CT contrast, the 10% NaBr brine was used for the water phase, and either *n*-hexane, *n*-octane, or *n*-decane was used for the oil phase. The core holders were standard Hassler type with an overburden fluid (water at 50 psi) and a rubber sleeve. The sand was packed into the rubber sleeve of 7.6 cm diameter and 67 cm length (87 cm sleeves were used for water-wet sand). The core was mounted onto a vertical positioning system in a Picker 1200X CT machine, which scanned in the horizontal plane. Scans of 5 mm width were taken every 2 cm along the core and at energy levels of 80 and 140 kV.

The experiment was calibrated by scanning the core when it was dry, when it was saturated with brine, and when it was saturated with oil. Using this calibration and a standard linear interpolation of the CT number (i.e., an attenuation coefficient), the water, oil, and air saturations could be obtained during a three-phase experiment. The saturations were observed to be uniform over each slice, except within 2 cm of the capillary fringe where the scans showed regions of high and low saturations. In either case, the saturations were averaged over each slice to give the average water, oil, and air saturation every 2 cm.

We can estimate the accuracy of the saturation by measuring the standard deviation on a pixel basis, and then assuming the standard deviation of the average saturation is the standard deviation of the mean. This gives a typical accuracy of $\Delta S_i \approx 0.0002$. This is likely to be too small due to nonlinear systematic variations such as beam hardening. In practice, when the core is at its initial condition with water and oil, but no gas, we measure a typical gas saturation value of $S_g \approx \pm 0.01$. Thus we estimate our accuracy for each phase to be $\Delta S_i \approx 0.01$.

Before drainage each core was set to connate water S_{wc} or residual oil S_{or} saturation as described earlier. Once the desired initial condition was reached, gas (air) was allowed to enter the top of the system, while water and oil drained out of the bottom under gravity. Before entering the column the air passed through a bubbler filled with water and a bubbler filled with oil to saturate the air with water and oil vapor. The bubblers also provided a one-way pathway for the air so that no oil and water vapor could leave the column through the top port. The height of oil and water that the entering air bubbled through was less than 1 cm, so the pressure boundary conditions were $P_g=0$ Pa at the outlet and $P_g \approx -100$ Pa at the inlet.

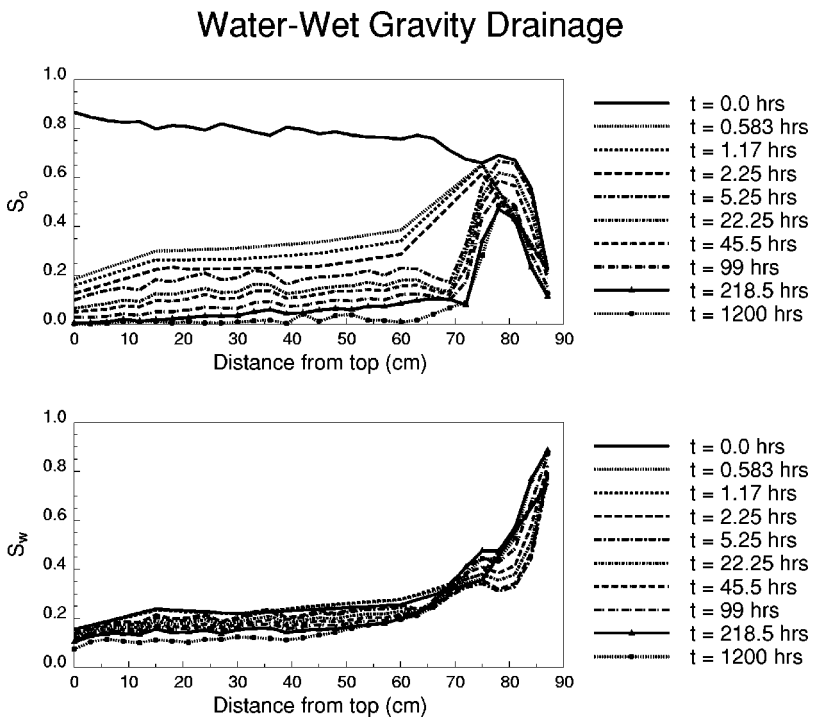

Fig. 1–Oil (octane) and water saturation profiles vs. time during gravity drainage. The sand was water-wet and the initial condition was connate water saturation S_{wc}. Oil and water permeabilities can be calculated directly from the measured distributions.

The pack was periodically scanned over a period of several weeks to record the saturation distribution vs. time. **Fig. 1** shows the saturation profile of octane and water at various times for a water-wet column that was initially at S_{wc}.

We can compute the oil and water relative permeabilities at each measured position along the column and for each time from the known time evolution of the saturation profile $S_i(z,t)$. We begin with Darcy's law for each phase in a one-dimensional vertical displacement,

$$u_i = -\frac{kk_{ri}}{\mu_i}\left(\frac{\partial P_i}{\partial z} - \rho_i g\right), \quad (3)$$

where u is the flux, k is the permeability (20 darcy for our sand), k_r is the relative permeability, μ is the viscosity, and z is the vertical distance taken to be positive downward. We calculate the flux past position z for time interval t_1, t_2 by integrating the change in the saturation of each phase between scans at times t_1 and t_2,

$$u_i(z,t_1,t_2) = \frac{\phi}{(t_2 - t_1)} \int_0^z S_i(z',t_1) - S_i(z',t_2)\mathrm{d}z', \quad (4)$$

where ϕ is the porosity.

The only remaining unknown is the pressure gradient ($\partial P_i/\partial z$). This can be found directly using tensiometers, or indirectly by calculating the pressures from the saturations and a known capillary pressure curve.[10] In practice the indirect method has difficulties for column positions near and below the capillary fringe since the quantity $\partial S_i/\partial z$ is large, and the capillary pressure gradient is very close to the gravitational gradient. Thus any small errors in the saturation measurement correspond to large errors in the measured permeability.

Fortunately, we notice that near the top of the column the saturation is roughly constant with position ($\partial S_i/\partial z \approx 0$). Thus we assume that $\partial P_i/\partial z \ll \rho_i g$ and ignore the capillary pressure gradient for positions over a region were the saturation data satisfy the above condition (between 20 and 50 cm in Fig. 1). For the shorter oil-wet, mixed-wet, and fractionally wet cores, the above condition was satisfied only between 10 and 30 cm from the top of the chamber. In essence, the CT scanner allows us to avoid capillary end effects in the determination of relative permeability, since we can choose a section over which the capillary pressure gradients are negligible compared to gravity.

For this region the relative permeability as a function of z and time interval t_1, t_2 can be found by combining Eqs. 3 and 4 and dropping the pressure gradient,

$$k_{ri}(z,t_1,t_2) = \frac{\mu_i \phi}{k\rho_i g(t_2 - t_1)} \int_0^z S_i(z',t_1) - S_i(z',t_2)\mathrm{d}z'. \quad (5)$$

Calculating the saturation as a function of z and time interval t_1, t_2 as the average of the t_1 and t_2 saturations,

$$S_i(z,t_1,t_2) = [S_i(z,t_1) + S_i(z,t_2)]/2, \quad (6)$$

we can then plot k_{ri} as a function of S_i.

The accuracy of the technique is a function of the accuracy of the saturations, fluxes, and pressure gradients. The saturation accuracy was estimated previously to be ± 0.01. The flux accuracy is also likely to be good, since we know the time accurately and, by integrating the saturations, the deviations are minimized further. The largest uncertainty is in the estimate of the pressure gradient. Simple two-phase simulations suggest that the assumption that the pressure gradient is small compared to the gravitational gradient is very good for short time scales (<2 weeks), but can be in error by up to 30% at long time scales (>6 weeks).

Gas Relative Permeability

We have developed a procedure to measure the gas relative permeability in the sand packs. Distilled water was used for the water phase, and *n*-octane for the oil phase. The sand is packed through a continuous pour into a 60 cm column made of 20 separate 3 cm long sections similar to that used in the capillary pressure curve measurements. Additionally, nine of the plastic sections in the column contain a small port through which the pressure of the gas phase can be measured. Thus we can measure eight separate pressure drops along the column during gas flow.

We first measure the single phase gas permeability by flowing known rates of CO_2 (between 5 and 10 mL/s) through the column and measuring the pressure drops across each section using a water manometer. For two-phase measurements, the column is then

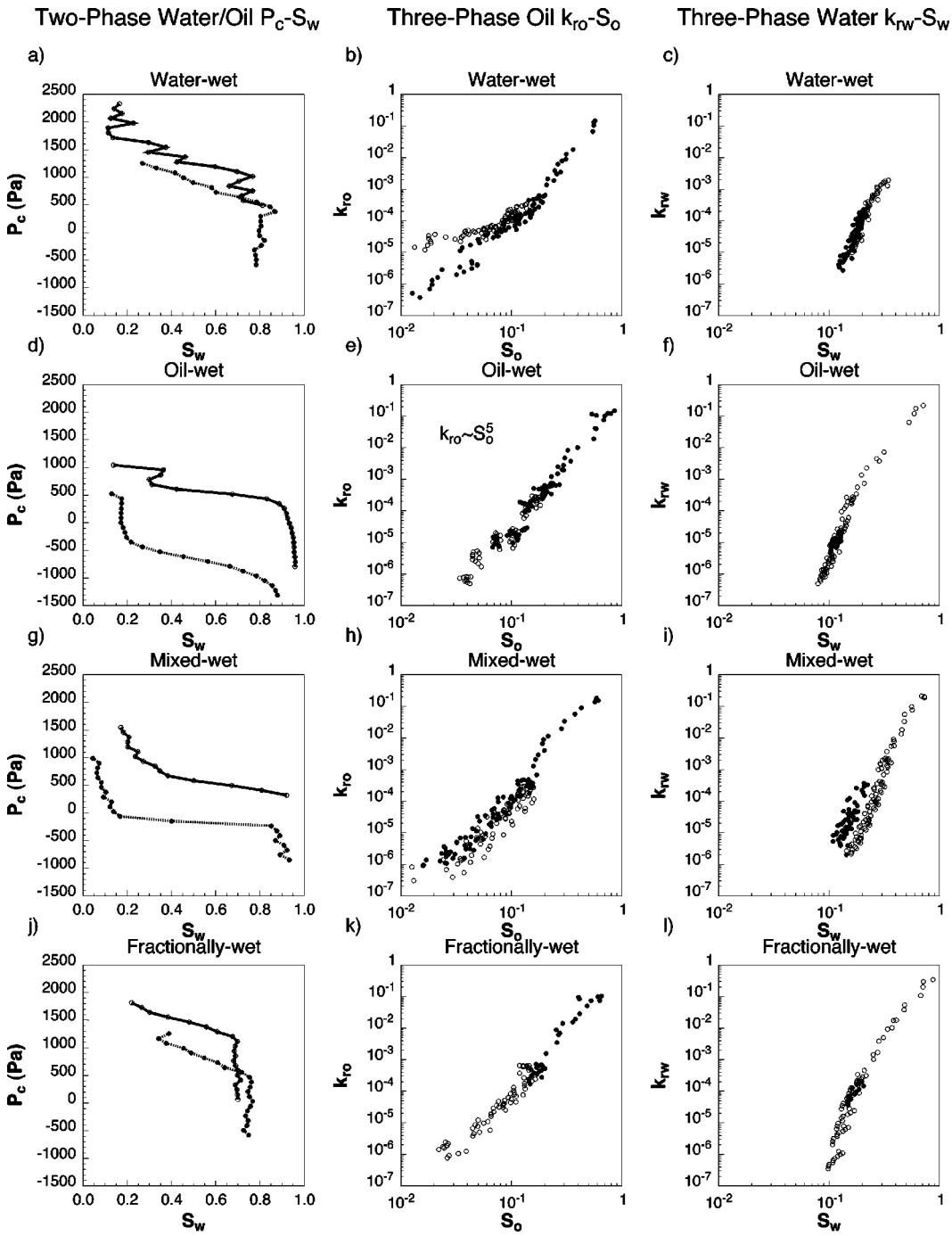

Fig. 2–Measured two-phase (water/oil) capillary pressure curves and three-phase oil and water relative permeabilities with *n*-octane as the oil for water-wet, oil-wet, mixed-wet, and fractionally wet sand. Open symbols denote drainages that started from residual oil saturation (S_{or}), and closed symbols denote drainages that started from connate water saturation (S_{wc}).

filled with de-gassed water from below and the water is circulated until all of the original CO_2 is displaced or dissolved. The column is then allowed to drain under gravity for about 1 hour, after which air is injected at a rate between 0.1 and 1 mL/s at the top of the column, displacing additional water out the bottom. This injection is continued for several hours until the pressures have stabilized and the gas and water phases are in equilibrium. Due to capillary effects, the distribution of water varies along the sand pack, with a high water saturation (and low gas saturation) near the outlet and a low water saturation (and high gas saturation) near the inlet. The pressure drop is measured between each section, which in turn gives the gas relative permeability. The column is sectioned and the water and gas saturations are obtained gravimetrically. Low injection rates retained more water in the column and were used for low gas saturation measurements. There was no measurable effect on the gas relative permeabilities from the different gas injection rates.

For three-phase measurements a nearly identical procedure is used. The only differences are (1) the column is first filled to S_{wc} and (2) the oil, water, and gas saturations are measured using the GC rather than gravimetrically. We did not measure the gas relative permeability for the mixed-wet sands.

Results

Capillary Pressure Curves. The first column of **Fig. 2** shows the drainage and imbibition curves for the sandpacks of different wettabilities. The curves are for two-phase water/oil displacements.

TABLE 2– AMOTT INDICES AND RESIDUAL SATURATIONS FROM THE TWO-PHASE (WATER/OIL) CAPILLARY PRESSURE CURVES

Wettability	I_w	I_o	S_{or}	S_{wc}
Water-wet	1	0	0.20	0.15
Oil-wet	0	0.05	0.05	0.20
Mixed wet	0.10	0	0.10	0.10
Fractionally wet	1.0	0	0.25	0.20

From these curves, the calculated Amott wettability indices[17] and two-phase residual saturations are shown in **Table 2**.

For the oil-wet medium, the procedure we used to make the oil-wet pack should produce a uniform wettability on all the pore surfaces. The large hysteresis compared to that of the water-wet case, the lack of spontaneous water imbibition, and the capillary pressures of the transition zones suggest that the water/oil contact angle is greater than 90°. Also, S_{or} is smaller than in the water-wet case, implying that the oil remains connected at low saturations.

Measurements of contact angles in glass capillary tubes that had been treated by crude oil in the same manner as our sand found an oil/water contact angle of 152°.[18] Contact angles this large in a porous medium should result in a significant degree of spontaneous oil imbibition.[19] However, the low oil Amott index of 0.05 shows that this is not the case. Overall, the oil-wet sandpack is only weakly oil-wet or almost neutrally wet. While a direct measurement of the oil/water contact angle on the sand grains is not possible, it is likely to be only slightly greater than 90°.

For the mixed-wet medium, we will assume that our procedure induced wettability changes like those described by Salathiel[20] and by Kovscek *et al.*[21] When the crude oil comes into contact with the solid, it can deposit surface active agents, rendering these surfaces oil-wet. The larger pore spaces will tend to be oil-wet, since the smaller pores and throats remain water filled. The corners and crevices of the large pore spaces will also remain water filled and thus water-wet. Thus the oil-wet and water-wet portions will be discriminated by pore size.

The irreducible water saturation, S_{wc} is slightly lower than in the water-wet sand, while the residual oil saturation, S_{or}, is between the water-wet and oil-wet cases. Also, the capillary pressures in the transition zone lie between the water-wet and oil-wet sands. The mixed-wet pack does not imbibe oil, but it does imbibe some water. Overall its Amott indices imply a weakly water-wet or neutrally wet system. It is possible that in our experiments the crude oil only renders the surfaces it contacts weakly oil-wet.

For the fractionally wet media, since each sand grain is either oil-wet or water-wet, each side of a pore will be either oil-wet or water-wet. There will be no pore size discrimination for oil-wet and water-wet portions. Also the oil-wet and water-wet surfaces will be connected only randomly, and will produce pockets of oil-wet and water-wet regions. This description agrees with the observed large residual water S_{wc} and large residual oil S_{or}, since each fluid can get trapped in its isolated pockets.[11] But the observed capillary pressures in the transition zones are much closer to the water-wet sands, which is unexpected.

Three-Phase Relative Permeability

Table 3 lists all the three-phase drainage experiments and the figures which display the data. The experiments studied how the three-phase relative permeabilities varied as a function of the oil phase, the porous medium, and the initial condition of the pack. The second and third columns in Fig. 2 show the measured relative permeabilities for oil and water for the water-wet, oil-wet, mixed-wet, and fractionally wet sandpacks with octane as the oil.

The open symbols are from the initial condition of S_{or} while the closed symbols are from drainages that started from initial condition S_{wc}. Note that we can measure saturations as low as $S=0.01$, with relative permeabilities spanning over six orders of magnitude. The observed scatter in the data is likely a result of a combination of uncertainty in the pressure gradient and the natural variations in the porous medium. For ease in viewing the data, each relative permeability (in this figure and the following figures) is shown as a function of only the particular phase's saturation. The relative permeability can also depend on how the rest of the pore space is partitioned between the other two fluids. This can appear as additional scatter in the above plots, and is discussed later.

Fig. 3 shows the measured oil relative permeability for hexane, octane, and decane in water-wet sand, and for octane in a water-wet consolidated sandstone.

Fig. 4 shows the measured water relative permeability for two-phase (gas/water) and three-phase drainages in water-wet sand.

Fig. 5 shows the measured gas relative permeabilities for (a) the two-phase gas/water system for different wettabilities and the two-phase gas/oil system for oil-wet media, and for (b) the three-phase system for water-wet and oil-wet media. Notice that for the gas permeability the plots are on linear axes.

The following features are observed in the measured relative permeabilities.

1. Except for the water in the mixed-wet sand, the oil and water relative permeabilities during three-phase drainage are independent of initial condition to within experimental scatter (Fig. 2).

2. The three-phase relative permeabilities of the most wetting fluid (water in water-wet media, oil in oil-wet media) and the

TABLE 3– DRAINAGE EXPERIMENTS FROM WHICH THREE-PHASE OIL AND WATER RELATIVE PERMEABILITIES WERE OBTAINED. THE COLUMN LABELED FIGURE SHOWS WHERE THE DATA ARE DISPLAYED. THE INITIAL CONDITION (I.C.) BEFORE DRAINAGE WAS EITHER WATERFLOOD RESIDUAL (S_{or}) OR CONNATE WATER (S_{wc})

Expt.	Figure(s)	Oil	Porous Medium	I.C.
1	1, 2, 3, 8	Octane	Water-wet sand	S_{wc}
2	2	Octane	Water-wet sand	S_{or}
4	3	Hexane	Water-wet sand	S_{wc}
5	3, 8	Decane	Water-wet sand	S_{wc}
6	3	Octane	Water-wet sandstone	S_{or}
7	2, 8	Octane	Oil-wet sand	S_{or}
8	2	Octane	Oil-wet sand	S_{wc}
9	2	Octane	Fractionally wet sand	S_{or}
10	2	Octane	Fractionally wet sand	S_{wc}
11	2	Octane	Mixed-wet sand	S_{or}
12	2	Octane	Mixed-wet sand	S_{wc}

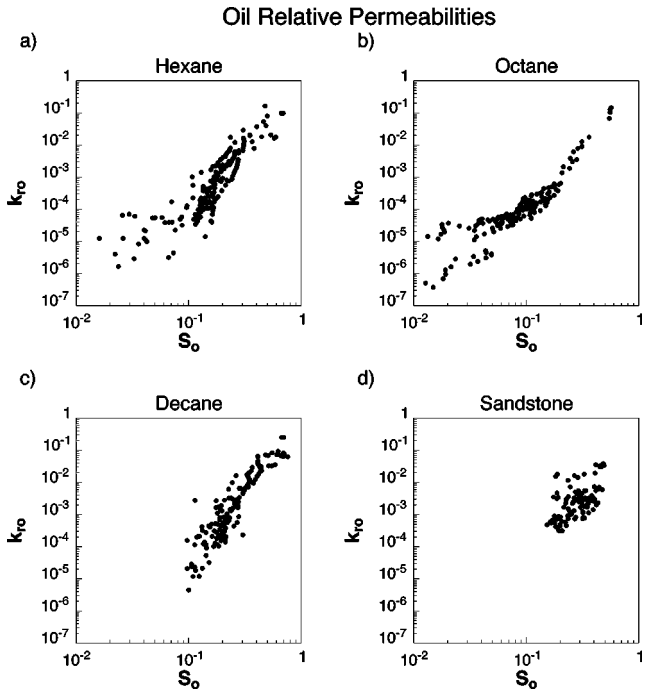

Fig. 3–Measured oil relative permeabilities with hexane, octane, and decane as the oil in water-wet sand and with octane in water-wet sandstone (Ref. 10) during three-phase gravity drainage.

two-phase water relative permeability in water-wet media are similar. All can be well described by a simple power law $k_r \sim S^{\alpha}$, where $\alpha \approx 5$ (Figs. 4a, 4b, 2c, and 2e). For the most-wetting fluid the permeability is the same for two- and three-phase displacements. However, for the most-wetting phase, a lower saturation is reached in the oil-wet medium (Fig. 2e) than in the water-wet medium (Fig. 2c).

3. At low saturations, $S < S_{or}\,(S_{wc})$, the relative permeabilities of oil in water-wet media (Fig. 2b) and water in oil-wet media (Fig. 2f) are very different. For hexane and octane, the oil relative permeability remains finite at low saturations with a power law of $k_r \sim S^{\alpha}$, where $\alpha \approx 2$ (Figs. 2b, 3a, and 3b). The water relative permeability drops off quickly, tending towards zero at water saturations of $S_w \approx 0.1$ (Fig. 2f).

4. For the mixed-wet sandpack, the oil relative permeability is similar to the water-wet sandpack at low saturations (Figs. 2h and 2b). It has the largest k_{ro} of any wettability at moderate saturations ($S_o = 0.2-0.4$). The water relative permeability is the smallest of all the wettabilities and it depended on the initial condition (Fig. 2i).

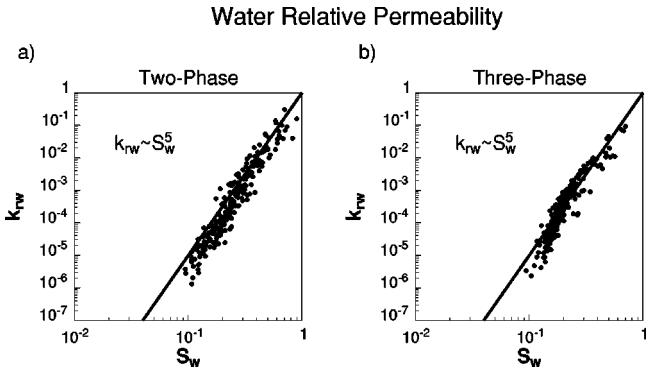

Fig. 4–Measured water relative permeabilities for (a) the two-phase (gas/water) system and (b) the three-phase (gas/oil/water) system from gravity drainages in water-wet sand.

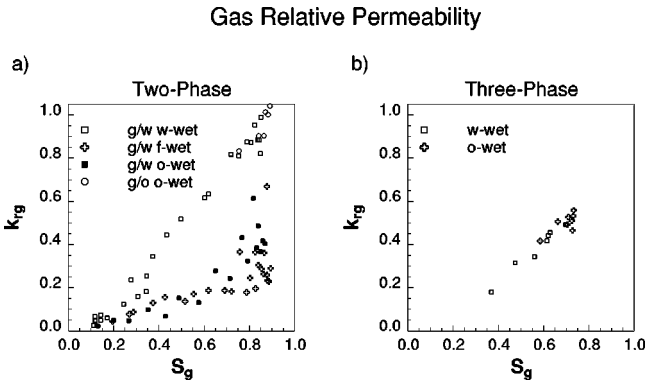

Fig. 5–Measured gas relative permeabilities for (a) the two-phase gas/water system for media of varying wettability and the two-phase gas/oil system for oil-wet media, and (b) the three-phase gas/oil/water system for water-wet and oil-wet media. The gas relative permeability in oil-wet sand is roughly a factor of 2 smaller than that for identical water-wet sand for two-phase gas/water systems.

5. When water is the main liquid phase, the gas relative permeability for the oil-wet and the fractionally wet medium is roughly a factor of 2 smaller than that for an identical water-wet medium (Fig. 5a). When oil is the main liquid phase, the gas relative permeability is independent of the wettability (Fig. 5a).

6. For the fractionally wet sandpack, the oil, water, and gas relative permeabilities are between the oil, water, and gas relative permeabilities in the water-wet and oil-wet sands (Figs. 2k, 2l, and 5a).

Although exact functional forms of relative permeabilities can be dependent on the specific porous medium, we believe that many of the above features are universal for three-phase displacements. We discuss this by considering the effects of pore-scale configuration on the relative permeabilities.

Pore-Scale Explanation

1. Except for the mixed-wet media, the oil and water relative permeabilities are independent of initial condition during three-phase drainage.

In water-wet media, the water occupies the smallest pores, regardless of the saturations of oil and gas. Thus in a drainage-type experiment with the water saturation decreasing, it is expected that the relative permeability of water is insensitive to initial condition. This behavior has been seen by other researchers.[6,22] Oil, however, occupies the intermediate sized pores, and its pore occupancy does depend on the saturations of both water and gas: in a gas/oil displacement, oil occupies the smaller pores, whereas for an oil/water displacement, oil occupies the larger pores. A review of the literature has shown that the oil relative permeability is sensitive to initial condition.[6,22] We do not see this for $S_o > 0.05$, and the oil relative permeability appears to be a function only of its own saturation. There is a significant effect of initial condition on k_{ro} for $S_o < 0.05$ in Fig. 2b. However, it is difficult to make a definitive comment because of considerable experimental inaccuracies in this low saturation region. The lack of sensitivity to initial condition at moderate oil saturations, could be due to the narrow pore size distribution of the sandpacks, and is consistent with other results in uniform media.[6,23] Similarly, for water in oil-wet media, we see no sensitivity to the initial condition, although the water is no longer the wetting phase.

In the mixed-wet media, we do see a measurable dependence on the initial condition for the water relative permeability. The water relative permeability is noticeably larger when starting from S_{wc} than from S_{or}. The water saturation does not drop below $S_w = 0.15$ when starting from S_{or}, while it reaches less than $S_w = 0.10$ when starting from S_{wc}. When the initial condition is S_{wc}, water is only present in the smaller pores and corners. In this sense it resembles a water-wet medium and, as can be seen in

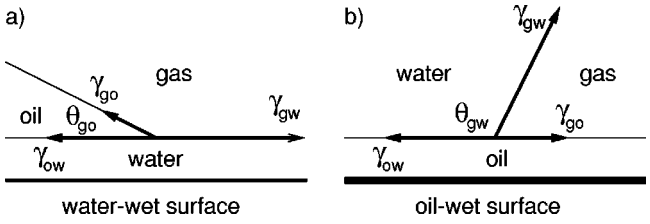

Fig. 6–Configuration of fluids on (a) a flat water-wet surface and (b) a flat oil-wet surface (shown in bold face).

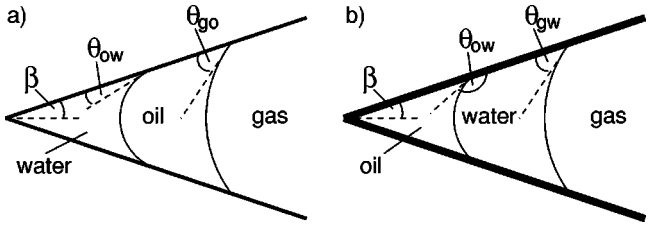

Fig. 7–Possible configuration of fluids in a pore space corner of half angle β: (a) water-wet surfaces and (b) oil-wet surfaces (shown in bold face). Note that configuration (b) is not allowed as $\theta_{gw}>90°$.

Figs. 2i and 2c, the water relative permeability is similar to the water-wet case. When drainage (gas invasion) starts from S_{or}, water is also present in the centers of larger pores. If these pores are oil-wet, then water can be trapped in them during drainage. In the oil-wet system, a residual water saturation of around $S_w = 0.10$ is observed (Fig. 2f). In the mixed-wet pack, the final water saturation is approximately $S_w = 0.15$, or the sum of the oil-wet residual and the remaining water saturation in the corners.

2. Similarity of the relative permeability of the most wetting phase in water-wet and oil-wet media.

The most-wetting phase occupies the smallest pores, and corners, grooves, and crevices in the wider pores. If we compare strongly and uniformly water-wet and oil-wet media, we would expect the configuration of the most-wetting fluid to be similar for both systems at the same saturation. The exact functional form of the relative permeability depends on the porous medium and is not universal. The only general feature is that k_r should asymptotically approach zero saturation at a sufficiently high capillary pressure, indicating that the wetting phase remains connected, albeit poorly, through wetting layers in crevices of the medium down to very low saturation.

In the experiments, the lowest-wetting phase saturation observed depends on the largest capillary pressure reached—it takes an infinite capillary pressure to reach zero saturation. It is possible to show[12] that at the top of the column smaller interfacial radii of curvature are achieved for oil in the oil-wet system than for water in the water-wet system. This explains why in our experiments the lowest water saturation reached in the water-wet pack ($S_w \approx 0.1$) is higher than that reached in the oil-wet pack ($S_o \approx 0.04$); see Fig. 2.

3. Very different forms for k_{ro} in water-wet media and k_{rw} in oil-wet media at low saturation.

At low saturation phases may remain connected through wetting layers in crevices in the pore space. It is this connectivity that controls k_r at low saturation. The pore-scale configuration and connectivity of oil and water are very different for water-wet and oil-wet media. Consider first the flat water-wet and oil-wet surfaces shown in **Fig. 6**.

The most-wetting fluid coats the surface. The contact angle between oil or water and gas, which will control the position of the phase in the pore space, is given by the balance of interfacial tensions, assuming that the solid is coated with a thick wetting film.

For oil in water-wet media (Fig. 6a)

$$\cos\theta_{go} = \frac{\gamma_{gw} - \gamma_{ow}}{\gamma_{go}} = 1 + \frac{C_{so}}{\gamma_{go}}, \quad (7)$$

where

$$C_{so} = \gamma_{gw} - \gamma_{ow} - \gamma_{go} \quad (8)$$

is the spreading coefficient for oil. Using our data in Table 1 we find $C_{so} = 3.5, -0.3$, and -3.1 mN/m for hexane, octane, and decane, respectively. For octane (the most used fluid) this results in $\theta_{go} \approx 10°$.

Now consider the three fluids in a corner of the pore space as shown in **Fig. 7a**. If $\theta_{ow} + \beta < 90°$ and $\theta_{go} + \beta < 90°$, where β is the half angle of the corner, then a layer of oil may be present.[2,24] These layers are on the order of micrometers thick and have been observed in micromodel experiments.[25-27] Drainage through oil layers is the mechanism by which very low oil saturations are reached during gas displacement in water-wet media.[3-5] Final oil saturations as low as $S_o = 0.001$ have been reached.[5] For a system with $\theta_{ow} = \theta_{go} = 0$, the oil layers can drain to infinitesimal thickness at a *finite* gas/oil capillary pressure, meaning that, in theory, $S_o = 0$ can be achieved through gravity drainage.[5,28] In our experiments the lowest saturation obtained is $S_o \approx 0.01$ after 7 weeks of drainage.

Displacement of oil below the waterflood residual oil saturation, S_{or}, requires layer drainage. In our experiments, and in others on bead packs, sandpacks and consolidated sandstones, a layer drainage regime consistent with $k_{ro} \sim S_o^2$ has been observed for $S_o < S_{or}$ (see Figs. 3a, 3b, and **8a**)[10,23,29]. This is readily explained by examining the flow in a single angular pore (see Fig. 7a). S_o is proportional to the area of the oil in the layer. The oil conductance for Poiseuille type flow is approximately proportional to the area squared, leading to $k_{ro} \sim S_o^2$.[2,30] This may seem a simple argument, but it is confirmed by a more detailed analysis of layer flow that has been verified against numerical solutions of the Navier-Stokes equation and experiments in square[30] and triangular[18] capillary tubes.

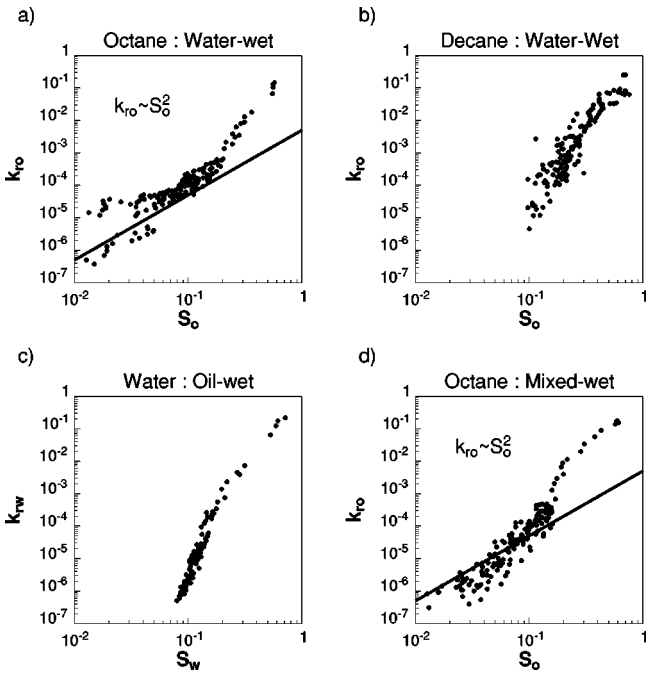

Fig. 8–Comparison of relative permeabilities. (a) A spreading system ($\theta_{go} \approx 0$): octane in water-wet sand. (b) A nonspreading system: decane in water-wet sand. (c) A nonwetting system: water in oil-wet sand. (d) A mixed-wet system: octane in mixed-wet sand. The solid lines in (a) and (d) show $k_{ro} \sim S_o^2$. The data, while consistent with this trend, only follow it approximately.

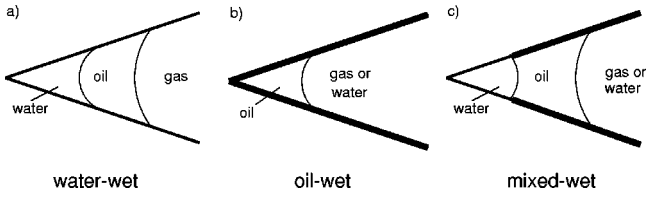

Fig. 9–Pore-scale arrangements of fluid for water-wet, oil-wet, and mixed-wet corners. A thick line represents an oil-wet surface. Notice that oil layers sandwiched between water and gas are present for both the water-wet and mixed-wet media, and this lead to similar k_{ro} at low S_o. In oil-wet media, oil is confined to the crevices and leads to a lower k_{ro}.

We observe layer drainage for a spreading system, loosely defined as one with $C_{so}\approx 0$, or $\theta_{go}\approx 0$. However, the situation is different for oils with a large and negative spreading coefficient.

For decane in water-wet media, our measurements of interfacial tension result in $\theta_{go}\approx 30°$. Decane layers have been seen in micromodels.[27] However, decane layers cannot form in oblique wedges ($\beta > 60°$), and are present for a more restricted range of capillary pressures than for octane.[2] If oil layers are not present, oil can be trapped, leaving a residual saturation at the end of drainage. In our experiments we do not observe a layer drainage regime in Fig. 8b.

For water in strongly oil-wet media (Fig. 6b),

$$\cos\theta_{gw}=\frac{\gamma_{go}-\gamma_{ow}}{\gamma_{gw}}=1+\frac{C_{sw}}{\gamma_{gw}}, \tag{9}$$

where

$$C_{sw}=\gamma_{go}-\gamma_{ow}-\gamma_{gw} \tag{10}$$

is the spreading coefficient for water. Using Table 1 we find $C_{sw}=-102.1$ mN/m and $\theta_{gw}\approx 115°$. Even if the surface is not strongly oil-wet, there is constraint between the interfacial tensions and contact angles,[30]

$$\gamma_{gw}\cos\theta_{gw}=\gamma_{ow}\cos\theta_{ow}+\gamma_{go}\cos\theta_{go}. \tag{11}$$

Using the octane data, if $\theta_{ow} > 110°$ then $\theta_{gw} > 90°$. Thus water is less wetting than gas, unless we have a very weakly oil-wet system ($\theta_{ow} < 110°$).

Measurements on oil-treated glass surfaces have found $\theta_{gw}=103°$, consistent with Eq. 9. In Fig. 7b, water layers can occur for $\theta_{gw}+\beta < 90°$, and gas layers can occur for $90°+\beta < \theta_{gw}$, neither of which is possible except for gas in exceptionally sharp crevices. The absence of a layer drainage regime is evident in Fig. 8c.

Note that k_{ro} for decane in a water-wet system is similar to k_{rw} in an oil-wet system. Both represent cases where the intermediate-wetting fluid is nonspreading and there is no layer drainage regime.

We do not observe the same layer drainage regime for the most wetting phase; instead of $k_r\sim S^2$, we observe $k_r\sim S^5$. The most wetting phase occupies the small pores and all the narrow nooks and crannies, where it is held by strong capillary forces and where it may be poorly connected. In contrast, oil layers in spreading systems reside over the water and, by construction therefore, are held by weaker capillary forces and are well connected throughout the porous medium.

4. The mixed-wet sandpack has a k_{ro} similar to the water-wet pack at low saturations, while it was the largest of any wettability at moderate saturations ($S_o=0.2-0.4$). k_{rw} is the smallest observed for any wettability.

Fig. 9 shows schematic arrangements of oil, water and gas in water-wet, oil-wet, and mixed-wet pores. In both water-wet and mixed-wet media water fills the corners of the pore space, even if oil fills the pore center. During gas injection, gas is nonwetting to oil, and thus in both cases layers of oil between water in the corners and gas in the pore centers may be present. As a consequence, k_{ro} at low S_o is similar for mixed-wet and water-wet media, with a characteristic layer drainage regime (Fig. 8d). This implies a possible universal form for k_{ro} at low S_o in mixed-wet reservoir settings, since the behavior is independent of the oil/water contact angle. Notice that the layers can form in a mixed-wet system, even if water is in the center of the pores. This agrees with the observations that k_{ro} at low saturations is independent of the initial condition even when more water is trapped in the pores when starting from S_{or}. In contrast, in uniformly oil-wet media, oil is confined to the corners. The oil is held by strong capillary forces and has a lower k_{ro} as discussed before.

Although it is difficult to see from the log-log plots of Fig. 2, between $S_o=0.2$ and 0.4, k_{ro} was noticeably the largest in the mixed-wet packs. In this saturation range, the fluids will be contacting both oil-wet and water-wet surfaces. This being said, it seems most likely that k_{ro} would be *smaller* than in the water-wet case, since the oil is most wetting on some of these surfaces. Thus, there is not a simple explanation of this phenomenon, although it would be interesting what behavior is seen in a three-phase, mixed-wet network model.

The low water relative permeability is due to the large trapped water saturation during drainage. As explained in explanation (1) in this section, this is greatest in mixed-wet packs, because the water can get trapped in the big pores, and held by capillary forces in the small pores.

5. When water is the main liquid phase, k_{rg} is lower in an oil-wet medium than in a water-wet medium.

For the two-phase gas/water system in water-wet media, the water phase will occupy the smallest pores and crevices while the gas phase occupies the large pore spaces. In oil-wet media, the contact angle is such that neither the water phase nor the gas phase wets the pore surfaces and thus the water and gas phases compete for the largest pores. Thus at equivalent gas saturations, in the oil-wet system the gas is in smaller pathways, leading to a lower permeability.

For the three-phase gas/oil/water system in water-wet media, the gas is nonwetting to both oil and water, so k_{rg} is expected to be a function only of gas saturation. In oil-wet media, gas is nonwetting to oil, but is not strongly nonwetting to water. Thus it is expected that in this case k_{rg} depends on both the oil and water saturations. From Fig. 5b we see that the three-phase k_{rg} in the oil-wet system is between the two-phase gas/water k_{rg} and gas/oil k_{rg}. Most three-phase models[6,22,31] assume that gas is always the nonwetting phase and k_{rg} is a function of gas saturation only, which is not supported by these measurements.

We also see that the three-phase k_{rg} in the water-wet system is lower than the two-phase water-wet gas/water k_{rg} and oil-wet gas/oil k_{rg}. Since the gas is the most nonwetting phase in all of these experiments, we expect the gas relative permeabilities to be similar. Why this is not the case is currently not known.

6. The fractionally wet sand has behavior intermediate between that of oil-wet and water-wet sand.

This last observation seems intuitively obvious. However, there are three important points to make. First, the oil in a spreading system is always connected regardless of the oil-wet fraction, since it can reside in corners as the most-wetting phase or in layers as the intermediate-wetting phase. Consistent with this is the observation that k_{ro} asymptotically approaches zero residual oil saturation for all wettabilities, as shown in Fig. 2. However, unless the small pores, corners, and crevices are completely water-wet, an infinite capillary pressure is required to achieve this. Second, note that the trapped water saturation for the fractionally wet sand is slightly *higher* than for the oil-wet sand. This is because in the fractionally wet sand, the oil-wet regions are poorly connected in the pack and this leads to significant trapping of water. This percolation-type argument has been explored in more detail by Zhou and Blunt.[11] Third, the gas relative permeability for the fractionally wet sand is very close to that in the oil-wet case. This shows that the gas mobility is significantly affected even if a fraction of the pores is oil-wet.

Discussion

Recently, there has been renewed interest in predicting capillary pressure curves and relative permeabilities from basic physics and from the pore structure using pore network models (see, for instance, Ref. 32). One of our objectives in this study was to obtain a complete data set (capillary pressure curves and relative permeabilities) as a function of wettability. We hope that these data can provide a benchmark with which to test the various three-phase, mixed-wettability network models now being proposed. In this vein, the data can all be found by following links from our web site: http://ekofisk.stanford.edu/supric.html/.

Conclusions

We used CT scanning and analog experiments to measure oil, water, and gas relative permeabilities during three-phase gravity drainage. Mixed-wet sandpacks were made by flooding a water-filled, water-wet pack with crude oil. The capillary pressure curve of the resultant medium indicated that it was neither strongly oil-wet nor water-wet. Drainage experiments were performed on oil-wet, water-wet, mixed-wet, and fractionally wet sandpacks. Saturations as low as 0.01 were recorded and the relative permeabilities span six orders of magnitude. The main results are the following.

1. At low oil saturations ($S_o < S_{or}$) in water-wet media, spreading systems show a characteristic form of the oil relative permeability with approximately $k_{ro} \sim S_o^2$. This is consistent with a theoretical interpretation of oil layer drainage at the pore scale. For a nonspreading decane system, the layer drainage regime was not observed.

2. Mixed-wet media also exhibit an approximate quadratic oil relative permeability at low oil saturations. The theoretical interpretation is that oil layers are present between water on the water-wet corners of the pore space and gas occupies the oil-wet center.

3. In oil-wet media, the oil relative permeability behaves similarly to the water relative permeability in water-wet systems. This is because in both cases we are considering the most-wetting phase.

4. In oil-wet media, the water has a large and negative spreading coefficient, meaning that water layers do not form in the pore space. The water relative pemeability k_{rw} for an oil-wet medium is similar to k_{ro} for a water-wet medium and a nonspreading oil.

5. In oil-wet media, the gas relative permeability is smaller than that for identical water-wet media. This is consistent with the gas and water phases competing for the largest pores in oil-wet media, where gas is not necessarily the nonwetting phase.

Nomenclature

C_{so} = spreading coefficient for oil, m/t^2, mN/m
C_{sw} = spreading coefficient for water, m/t^2, mN/m
I_o = Amott oil index, dimensionless
I_w = Amott water index, dimensionless
g = gravitational constant, L/t^2, m/s^2
K = permeability, L^2, darcy
k_{ri} = relative permeability to phase i, dimensionless
P_c = capillary pressure, m/Lt^2, Pa
P_i = pressure of phase i, m/Lt^2, Pa
S_i = saturation of phase i, dimensionless
S_{or} = waterflood residual oil saturation, dimensionless
S_{wc} = connate water saturation, dimensionless
u_i = flux of phase i, L/t, m/s

Greek Letters

α = power law exponent, dimensionless
β = half angle of pore corner, dimensionless
γ_{ow} = oil/water interfacial tension, m/t^2, mN/m
γ_{go} = gas/oil interfacial tension, m/t^2, mN/m
γ_{gw} = gas/water interfacial tension, m/t^2, mN/m
μ_i = viscosity of fluid i, m/Lt, cp
ϕ = porosity, dimensionless
ρ_i = density of fluid i, m/L^3, kg/m^3
θ_{ow} = oil/water contact angle, dimensionless
θ_{go} = gas/oil contact angle, dimensionless
θ_{gw} = gas/water contact angle, dimensionless

Subscripts

i = phase
g = gas
o = oil
w = water (brine)

Acknowledgments

We thank Jill Buckley for helpful discussions, Tuba Firincioglu, Huda Nassori, Will Whitted, and Jaime Hardt for experimental assistance, and Tom Lutz of Thums Inc. for supplying the crude oil. We gratefully acknowledge financial support from the members of the Stanford U. Gas Injection Affiliates Program (SUPRI-C) and from the Dept. of Energy under Grant No. DE-FG22-96BC14851.

References

1. Skauge, A. *et al.*: ''Influence of Connate Water on Oil Recovery by Gravity Drainage,'' paper SPE 27817 presented at the SPE/DOE 1994 Symposium on Improved Oil Recovery, Tulsa, Oklahoma, 17–20 April.
2. Fenwick, D.H. and Blunt, M.J.: ''Network Modeling of Three-Phase Flow in Porous Media,'' *SPEJ* (March 1998) 86.
3. Dumoré, J.M. and Schols, R.S.: ''Drainage Capillary-Pressure Functions and the Influence of Connate Water,'' *SPEJ* (October 1974) 437.
4. Kantzas, A., Chatzis, I., and Dullien, F.A.L.: ''Enhanced Oil Recovery by Inert Gas Injection,'' paper SPE 17379 presented at the 1988 SPE/DOE Symposium on Enhanced Oil Recovery, Tulsa, Oklahoma, 17–20 April.
5. Zhou, D. and Blunt, M.J.: ''Effect of Spreading Coefficient on the Distribution of Light Non-Aqueous Phase Liquid in the Subsurface,'' *J. Contam. Hydrol.* (1997) **25**, 1.
6. Baker, L.E.: ''Three-Phase Relative Permeability Correlations,'' paper SPE 17369 presented at the 1998 SPE/DOE Symposium on Enhanced Oil Recovery, Tulsa, Oklahoma, 17–20 April.
7. Oak, M.J., Baker, L.E., and Thomas, D.C.: ''Three-Phase Relative Permeability of Berea Sandstone,'' *JPT* (August 1990) 1054; *Trans.*, AIME, **289**.
8. Vizika, O. and Lombard, J.-M.: ''Wettability and Spreading: Two Key Parameters in Oil Recovery With Three-Phase Gravity Drainage,'' *SPERE* (February 1996) 54.
9. Jerauld, G.R.: ''Prudhoe Bay Gas/Oil Relative Permeability,'' *SPERE* (February 1997) 66.
10. Sahni, A., Burger, J.E., and Blunt, M.J.: ''Measurement of Three Phase Relative Permeability During Gravity Drainage Using CT Scanning,'' paper SPE 39655 presented at the 1998 SPE/DOE Improved Oil Recovery Symposium, Tulsa, Oklahoma, 19–22 April.
11. Zhou, D. and Blunt, M.J.: ''Wettability Effects in Three-Phase Gravity Drainage,'' *J. Pet. Sci. Eng.* (1998) **20**, 203.
12. DiCarlo, D.A., Sahni, A., and Blunt, M.J.: ''The Effect of Wettability on Three-Phase Relative Permeability,'' *Transp. Porous Media* (to be published).
13. Buckley, J.S. and Liu, Y.: ''Some Mechanisms of Crude Oil/Brine/Solid Interactions,'' *J. Pet. Sci. Eng.* (1998) **20**, 155.
14. Buckley, J.S. *et al.*: ''Asphaltenes and Crude Oil Wetting—The Effect of Oil Composition,'' *SPEJ* (June 1997) 107.
15. *CRC Handbook of Chemistry and Physics*, 62nd edition, Weast, R.C. and Astle, M.J. (eds.), CRC Press Inc., Boca Raton, FL (1981).
16. Adamson, A.W.: *Physical Chemistry of Surfaces*, fifth edition, John Wiley and Sons, New York City (1990).
17. Amott, E.: ''Observations Relating to the Wettability of a Porous Rock,'' *Trans.*, AIME (1955) **216**, 156.
18. Firincioglu, T., Blunt, M.J., and Zhou, D.: ''Three-Phase Flow and Wettability Effects in Triangular Capillaries,'' *Colloids Surf., A* (1999) **155**, 259.
19. Dullien, F.A.L.: *Porous Media: Fluid Transport and Pore Structure*, second edition, Academic Press, San Diego (1992).
20. Salathiel, R.A.: ''Oil Recovery by Surface Film Drainage in Mixed-Wettability Rocks,'' *JPT* (October 1973) 1216; *Trans.*, AIME, **255**.
21. Kovscek, A.R., Wong, H., and Radke, C.J.: ''A Pore-Level Scenario for the Devolpment of Mixed Wettability in Oil Reservoirs,'' *AIChE. J.* (1993) **39**, 1072.

22. Fayers, F.J. and Matthews, J.D.: ''Evaluation of Normalized Stone's Methods for Estimating Three-Phase Relative Permeabilities,'' *SPEJ* (April 1984) 224; *Trans.*, AIME, **277**.
23. Grader, A.S. and O'Meara, D.J. Jr.: ''Dynamic Displacement Measurements of Three-Phase Relative Permeabilities Using Three Immiscible Liquids,'' paper SPE 18293 presented at the SPE Annual Technical Conference and Exhibition, Houston, 2–5 October.
24. Øren, P.-E. and Pinczewski, W.V.: ''Fluid Distribution and Pore Scale Displacement Mechanisms in Drainage Dominated Three Phase Flow,'' *Transp. Porous Media* (1995) **20**, 105.
25. Øren, P.-E., Billiote, J., and Pinczewski, W.V.: ''Mobilization of Waterflood Residual Oil by Gas Injection for Water Wet Conditions,'' *SPEFE* (March 1992) 70; *Trans.*, AIME, **293**.
26. Soll, W.E., Celia, M.A., and Wilson, J.L.: ''Micromodel Studies of Three-Fluid Porous Media Systems: Pore-Scale Processes Relating To Capillary Pressure-Saturation Relationships'' *Water Resour. Res.* (1993) **29**, 2963.
27. Keller, A.A., Blunt, M.J., and Roberts, P.V.: ''Micromodel Observation of the Role of Oil Layers in Three Phase Flow,'' *Transp. Porous Media* (1997) **26**, 277.
28. Blunt, M.J., Zhou, D., and Fenwick, D.H.: ''Three Phase Flow and Gravity Drainage in Porous Media,'' *Transp. Porous Media* (1995) **20**, 77.
29. Naylor, P. *et al.*: ''Gravity Drainage During Gas Injection,'' Proceedings of the 1995 European IOR-Symposium, Vienna, Austria, 15–17 May.
30. Zhou, D., Blunt, M.J., and Orr, F.M. Jr.: ''Hydrocarbon Drainage Along Corners of Noncircular Capillaries,'' *J. Colloid Interface Sci.* (1997) **187**, 11.
31. Stone, H.L.: ''Probability Model for Estimating Three-Phase Relative Permeability,'' *JPT* (February 1970) 214; *Trans.*, AIME, **249**.
32. Øren, P.-E., Bakke, S., and Arntzen, O.J.: ''Extending Predictive Capabilities to Network Models,'' *SPEJ* (December 1998) 324.

SI Metric Conversion Factors

cp × 1.0*	E−03 = Pa·s
darcy × 9.87	E−13 = m^2

*Conversion factor is exact.

SPEJ

David A. DiCario is Acting Assistant Professor in the Petroleum Engineering Dept. of Stanford U., Stanford, California. e-mail: dicarlo@pangea.stanford.edu. His research interests include multiphase flow in porous and fractured media, preferential flow, and environmental problems. Before joining the Stanford faculty, he worked in the Dept. of Agricultural and Biological Engineering at Cornell U. DiCarlo holds MS and PhD degrees in experimental physics from Cornell U. **Akshay Sahni** is a research scientist with Chevron Petroleum Technology Co. in San Ramon, California. Previously, he was a doctoral candidate in the Petroleum Engineering Dept. at Stanford U. His research interests are in multiphase flow in porous media, heavy-oil recovery, and pressure-transient analysis. Sahni holds an MS degree from the U. of Alaska, Fairbanks, and a PhD degree from Stanford U., both in petroleum engineering. **Martin J. Blunt** is Professor of Petroleum Engineering and head of the Petroleum Engineering and Rock Mechanics Research Group at Imperial College, London. He previously was an associate professor at Stanford U. and worked at the BP Research Center. He holds MA and PhD degrees in physics from Cambridge U. Blunt, winner of the 1996 Cedric K. Ferguson Medal, served as Associate Editor of *SPE Journal* during 1996-98. He currently is a member of the Editorial Review Committee and the Improved Oil Recovery Symposium Program Committee.